On the Robustness of Spatial Modulation to I/Q Imbalance

Ahmed G. Helmy, Marco Di Renzo, and Naofal Al-Dhahir

***Abstract*— We analyze the bit error rate performance of spatial modulation (SM)-based direct-conversion transceivers under transmit in-phase/quadrature (I/Q) imbalance. To investigate the impact of transmit I/Q imbalance on SM, we derive the signal-to-noise ratio loss due to I/Q imbalance impact compared with an ideal direct-conversion transceiver with no I/Q imbalance. Our analysis unveils the robustness of SM to transmit I/Q imbalance compared with conventional single-input multi-output transmissions, by relying more on the spatial domain.**

***Index Terms*— Spatial Modulation, MIMO, I/Q imbalance, Internet of Things.**

I. Introduction

THE significant increase in the deployment of Internet-of-Things (IoT) devices and wearables highlights the critical need for innovative physical layer waveform designs with higher energy and spectral efficiencies and lower-complexity transceivers. IoT devices have design constraints and performance requirements that differ from sensor networks and mobile terminals. Sensors must be very cheap, tiny, energy-efficient and are used for low data-rate applications. Mobile terminals are designed for higher data-rate applications and their energy consumption constraints are more relaxed than sensors. Hence, sensors are usually equipped with a single radio frequency (RF) chain and a single transmit antenna, while mobile terminals can accommodate multiple RF chains and antennas. IoT devices have characteristics and requirements in between those of sensors and mobile terminals [1].

Spatial Modulation (SM) was proposed to improve the energy and spectral efficiencies by activating only one transmit antenna and using its index as part of the information bits [2]. The high potential of SM in dense low-power IoT networks is motivated by [2] which showed that conventional multi-input multi-output (MIMO) transceivers suffer from a significant energy inefficiency compared to single-antenna transceivers due to the increased power dissipated by all of the RF chains.

MIMO wireless transceivers typically use the direct-conversion architecture, to enable small-form-factor low-power implementations. However, direct-conversion wireless transceivers suffer from several major RF impairments which limit their performance [3] such as I/Q imbalance which is due to any mismatch between the In-phase (I) and Quadrature-phase (Q) branches from the ideal case, *i.e.*, from the equal amplitudes and the exact 90° phase. For IoT and wearable devices, the I/Q imbalance will be even more pronounced due to the use of cost-constrained analog components, such as mixers and phase shifters in their RF front-ends. Since some of the information bits in SM are transmitted via the index of the activated transmit antenna, both transmit and receive I/Q imbalance affect the receiver's capability of detecting the correct active transmit antenna index as the I/Q imbalance can modify the channel signature significantly. This effect is added to the well-known sensitivity of the signal constellation domain to I/Q imbalance as in conventional single-input multi-output (SIMO) or MIMO transceivers [3]. The impact of the I/Q imbalance on SM-based MIMO transmission was firstly investigated in [4], [5] by analyzing the bit-error rate (BER) performance of SM under I/Q imbalance. References [4] and [5], however, do not provide a mathematical proof of the robustness of SM to I/Q imbalance compared to conventional SIMO/MIMO transceivers. In this letter, we propose a simple and insightful mathematical framework that proves the robustness of SM as a function of the system parameters and explicitly highlights the role played by the spatial constellation diagram in minimizing the impact of I/Q imbalance in SM. More specifically, our main contributions are as follows

- We derive a closed-form expression for the BER union bound of SM under transmit I/Q imbalance.
- We propose an analytical framework that decomposes the signal-to-noise ratio (SNR) loss due to transmit I/Q imbalance into three terms where the first term depends on the transmit I/Q imbalance parameters only, the second term depends only on the signal domain, while the third term depends on both the signal and spatial domains.
- We show analytically and by simulations that SM can reduce the well-known sensitivity of the signal constellation domain to transmit I/Q imbalance, in conventional SIMO transceivers, by relying more on the spatial domain especially for higher spectral efficiencies. This key result motivates SM for IoT devices.

Notation: We denote the Hermitian, *i.e.* complex-conjugate transpose of a matrix or a vector, by $(\cdot)^H$. The conjugate of a matrix, a vector, or a scalar is denoted by $(\cdot)^*$.

II. System Model Under I/Q Imbalance

We consider an SM-based uplink MIMO system where an IoT device equipped with N_T transmit antennas where only a single antenna is active in each transmission interval to communicate with a data sink receiver equipped with N_R receive antennas [2]. Assuming a spectral efficiency of m bps/Hz, each m-bit block is divided into two parts: (1) the data bits $m_d = \log_2 M$ derived from a size-M complex signal constellation Ψ and (2) the active antenna selection bits $m_a = \log_2 N_T$ derived from the space constellation which

Manuscript received December 19, 2016; revised January 9, 2017 and February 2, 2017; accepted February 28, 2017. Date of publication March 2, 2017; date of current version July 8, 2017. This publication was made possible by NPRP grant # 8-627-2-260 from the Qatar National Research Fund (a member of Qatar Foundation). The statements made herein are solely the responsibility of the authors. The associate editor coordinating the review of this letter and approving it for publication was T. Ngatched. *(Corresponding author: Ahmed G. Helmy)*

A. G. Helmy and N. Al-Dhahir are with the Department of Electrical Engineering, The University of Texas at Dallas, Richardson, TX 75080 USA (e-mail: ahmed.g.helmy@utdallas.edu; aldhahir@utdallas.edu).

M. Di Renzo is with the Laboratory of Signals and Systems, CentraleSupélec, University Paris-Sud XI, 91405 Orsay, France (e-mail: marco.direnzo@lss.supelec.fr).

Digital Object Identifier 10.1109/LCOMM.2017.2677421

represents the index of the active transmit antenna [2]. The $N_T \times 1$ all-zero vector $\mathbf{x}_i(s_l)$ contains only a single non-zero entry s_l at the i-th location which corresponds to the i-th active transmit antenna ($i.e.\ i = 1, \cdots, N_T$) where s_l is the complex transmitted symbol ($i.e.\ l = 1, \cdots, M$) [2] and $m = m_d + m_a$. The I/Q Imbalance-free $N_R \times 1$ received signal vector $\mathbf{y} = \mathbf{H}\mathbf{x}_i(s_l) + \mathbf{n} = \mathbf{h}_i s_l + \mathbf{n}$ where $\mathbf{H}$ is the $N_R \times N_T$ channel matrix whose entries are assumed to be independent and identically-distributed (i.i.d) quasi-static Rayleigh fading with unit variance and $\mathbf{n}$ is the $N_R \times 1$ complex additive white Gaussian noise (AWGN) vector with covariance matrix $\sigma^2\mathbf{I}_{N_R}$.

We start from the joint transmit-receive I/Q imbalance model in [3] where the received signal vector $\tilde{\mathbf{y}}$ under joint TX-RX I/Q imbalance is given by

$$\begin{aligned}\tilde{\mathbf{y}} &= \underbrace{\begin{bmatrix}\mu_R\mathbf{I}_{N_R} & \nu_R\mathbf{I}_{N_R}\end{bmatrix}}_{\mathbf{A}^H} \\ &\times \left\{ \underbrace{\begin{bmatrix}\mathbf{H} & 0\\ 0 & \mathbf{H}^*\end{bmatrix}}_{\tilde{\mathbf{H}}} \underbrace{\begin{bmatrix}\mu_T\mathbf{I}_{N_T} & \nu_T\mathbf{I}_{N_T}\\ \nu_T^*\mathbf{I}_{N_T} & \mu_T^*\mathbf{I}_{N_T}\end{bmatrix}}_{\mathbf{B}\otimes\mathbf{I}_{N_T}} \underbrace{\begin{bmatrix}\mathbf{x}_i(s_l)\\ \mathbf{x}_i^*(s_l)\end{bmatrix}}_{\tilde{\mathbf{x}}_i(s_l)} + \underbrace{\begin{bmatrix}\mathbf{n}\\ \mathbf{n}^*\end{bmatrix}}_{\tilde{\mathbf{n}}} \right\} \\ &= \tilde{\mathbf{H}}_{eq}\tilde{\mathbf{x}}_i(s_l) + \tilde{\mathbf{n}}_{eq} = \tilde{\mathbf{H}}_{eq}^{(i)}\mathbf{s}_l + \tilde{\mathbf{n}}_{eq}, \end{aligned} \quad (1)$$

where $\mu_{T/R}$, $\nu_{T/R}$ are the TX-RX I/Q imbalance parameters defined in [7] and $\mathbf{I}_q$ is an identity matrix of size q.

$\tilde{\mathbf{H}}_{eq}$ in Eq. (1) is the $N_R \times 2N_T$ equivalent channel matrix, including TX-RX I/Q imbalance effects, given by $\tilde{\mathbf{H}}_{eq} = \mathbf{A}^H\tilde{\mathbf{H}}\left(\mathbf{B}\otimes\mathbf{I}_{\mathbf{N_T}}\right)$ and the matrices $\mathbf{A}$ and $\tilde{\mathbf{H}}$ are defined in Eq. (1) where $\mathbf{B} = \begin{bmatrix}\mu_T & \nu_T\\ \nu_T^* & \mu_T^*\end{bmatrix}$. The matrix $\tilde{\mathbf{H}}_{eq}^{(i)}$ is the $N_R \times 2$ equivalent channel matrix corresponding to the i-th active transmit antenna ($i.e.$ columns i and $(i+N_T)$ of $\tilde{\mathbf{H}}_{eq}$). The vector $\mathbf{s}_l$ is defined as $\mathbf{s}_l = \begin{bmatrix}s_l & s_l^*\end{bmatrix}^T$ and the AWGN equivalent noise vector $\tilde{\mathbf{n}}_{eq} = \mathbf{A}^H\tilde{\mathbf{n}}$ where $\tilde{\mathbf{n}}$ is defined in Eq. (1).

III. BER Performance Analysis Under I/Q Imbalance

We consider the maximum likelihood (ML) detector as defined in [2]. Assuming that the channel matrix and the RX I/Q imbalance parameters are perfectly known at the receiver side (e.g. estimated using training symbols and during the calibration processing as shown in [6]), the RX I/Q imbalance can be completely eliminated from the received signal $\mathbf{z}$ using the widely-linear pre-processing operation [7]

$$\mathbf{z} = \left[\tilde{\mathbf{y}} - \left(\nu_R/\mu_R^*\right)\tilde{\mathbf{y}}^*\right] / \left[\mu_R - \left(|\nu_R|^2/\mu_R^*\right)\right], \quad (2)$$

where $\mathbf{z} = \overline{\mathbf{H}}_{eq}\tilde{\mathbf{x}}_i(s_l) + \bar{\mathbf{n}}_{eq} = \overline{\mathbf{H}}_{eq}^{(i)}\mathbf{s}_l + \bar{\mathbf{n}}_{eq}$. It is straightforward to show that $\overline{\mathbf{H}}_{eq} = \begin{bmatrix}\mathbf{I}_{N_R} & \mathbf{0}_{N_R}\end{bmatrix}\tilde{\mathbf{H}}\left(\mathbf{B}\otimes\mathbf{I}_{\mathbf{N_T}}\right)$ and $\bar{\mathbf{n}}_{eq} = \begin{bmatrix}\mathbf{I}_{N_R} & \mathbf{0}_{N_R}\end{bmatrix}\tilde{\mathbf{n}}$. Our assumption of fully-compensated RX I/Q imbalance is reasonable in practice especially for our assumed uplink model where the I/Q imbalance at the data sink receiver is typically small compared to that of the IoT device. **Henceforth, I/Q imbalance refers to TX I/Q imbalance only**. The I/Q imbalance-aware ML detector that jointly detects the optimal active transmit antenna index $\hat{i}$ and the complex signal symbol vector $\hat{\mathbf{s}}_l$ is defined as follows

$$\left\{\hat{i}, \hat{\mathbf{s}}_l\right\} = \underset{\mathbf{s}_l\in\Psi,\ i=1,\cdots,N_T}{\arg\min} \left\|\mathbf{z} - \overline{\mathbf{H}}_{eq}^{(i)}\mathbf{s}_l\right\|_2^2, \quad (3)$$

where $\hat{\mathbf{s}}_l = \begin{bmatrix}\hat{s}_l & \hat{s}_l^*\end{bmatrix}^T$. The BER P_e can be approximated via the union bound as follows [8]

$$\begin{aligned}P_e \le \frac{1}{m2^m}\sum_{i=1}^{N_T}\sum_{l=1}^{M}\sum_{i'\neq i}^{N_T}\sum_{l'\neq l}^{M} \mathrm{d}\left((i,l),(i',l')\right) \\ \times \mathrm{P}\left(\tilde{\mathbf{x}}_i(s_l) \to \tilde{\mathbf{x}}_{i'}(s_{l'})\right),\end{aligned} \quad (4)$$

where $\mathrm{P}\left(\tilde{\mathbf{x}}_i(s_l) \to \tilde{\mathbf{x}}_{i'}(s_{l'})\right)$ is the pairwise error probability (PEP) which is the probability that the transmitted vector $\tilde{\mathbf{x}}_i(s_l)$ is erroneously decoded as $\tilde{\mathbf{x}}_{i'}(s_{l'})$ and $m = \log_2(N_T M)$. In addition, $d\left((i,l),(i',l')\right)$ is the Hamming distance determined by the number of erroneous bits between $\tilde{\mathbf{x}}_i(s_l)$ and $\tilde{\mathbf{x}}_{i'}(s_{l'})$. Adopting the ML detector, an error $\tilde{\mathbf{x}}_i(s_l) \to \tilde{\mathbf{x}}_{i'}(s_{l'})$ occurs when $\left\|\mathbf{z} - \overline{\mathbf{H}}_{eq}\tilde{\mathbf{x}}_i(s_l)\right\|_2^2 > \left\|\mathbf{z} - \overline{\mathbf{H}}_{eq}\tilde{\mathbf{x}}_{i'}(s_{l'})\right\|_2^2$.

Based on the analytical framework in [9], the PEP conditioned on $\overline{\mathbf{H}}_{eq}$ can be expressed as

$$\mathrm{P}\left(\tilde{\mathbf{x}}_i(s_l) \to \tilde{\mathbf{x}}_{i'}(s_{l'}) \,|\overline{\mathbf{H}}_{eq}\right) = Q\left(\sqrt{\frac{\left\|\overline{\mathbf{H}}_{eq}^{(i)}\mathbf{s}_l - \overline{\mathbf{H}}_{eq}^{(i')}\mathbf{s}_{l'}\right\|_2^2}{4\sigma^2}}\right), \quad (5)$$

where $Q(.)$ is the Gaussian Q-function. Averaging over the distribution of $\overline{\mathbf{H}}_{eq}$ and using the alternative definition of the Q-function in [9], the unconditional PEP is given by

$$\mathrm{P}\left(\tilde{\mathbf{x}}_i(s_l) \to \tilde{\mathbf{x}}_{i'}(s_{l'})\right) = \frac{1}{\pi}\int_0^{\frac{\pi}{2}} \Phi_t\left(-\frac{1}{8\sigma^2 sin^2\theta}\right) d\theta, \quad (6)$$

where $\Phi_t(\vartheta)$ denotes the moment generating function (MGF) of the random variable $t = \left\|\overline{\mathbf{H}}_{eq}^{(i)}\mathbf{s}_l - \overline{\mathbf{H}}_{eq}^{(i')}\mathbf{s}_{l'}\right\|_2^2$.

To better understand the impact of TX I/Q imbalance on the spatial and the signal constellation components, we follow the approach in [10] to decompose the BER union bound as a summation of the following three terms

1) a term that characterizes the effect of TX I/Q imbalance *only* in the signal domain, denoted by P_e^{signal};
2) a term that characterizes the effect of the TX I/Q imbalance *only* in the spatial domain, denoted by $P_e^{spatial}$;
3) a joint term that characterizes the effect of the TX I/Q imbalance on *both* the signal and the spatial domains, denoted by P_e^{joint}.

Based on the definition of $d\left((i,l),(i',l')\right)$ between $\tilde{\mathbf{x}}_i(s_l)$ and $\tilde{\mathbf{x}}_{i'}(s_{l'})$, the erroneous bits may result from the incorrect detection of the antenna index i or the signal constellation symbol $\mathbf{s}_l$ or both. The three components of the BER union bound in Eq. (15) are obtained as follows

1) P_e^{signal} results from summing all terms in Eq. (4) where $i = i'$ and $l \neq l'$. Hence, the Hamming distance $d\left((i,l),(i',l')\right)$ and the random variable t are reduced to $d\left(l,l'\right)$ and $t = \left\|\overline{\mathbf{H}}_{eq}^{(i)}\left(\mathbf{s}_l - \mathbf{s}_{l'}\right)\right\|_2^2$, respectively. Following [11], the MGF of the random variable t is given by $\Phi_t(\vartheta) = \left(1 - \vartheta\varphi_{l,l'}\right)^{-N_R}$ where $\varphi_{l,l'} = \|\mathrm{B}\left(\mathbf{s}_l - \mathbf{s}_{l'}\right)\|_2^2$. Therefore, P_e^{signal} is given by

$$P_e^{signal} = \sum_{l=1}^{M}\sum_{l'\neq l}^{M} \frac{\mathrm{d}\left(l,l'\right)}{M\log_2(N_T M)}\beta\left(\frac{\varphi_{l,l'}}{8\sigma^2}\right), \quad (7)$$

where

$$\beta(x) = [g(x)]^{N_R} \times \sum_{\kappa=0}^{N_R-1} \frac{(N_R-1+\kappa)!}{\kappa!\,(N_R-1)!}\,[1-g(x)]^{\kappa} \quad (8)$$

$$g(x) = \frac{1}{2}\left(1-\sqrt{\frac{x}{1+x}}\right). \quad (9)$$

For high SNR, P_e^{signal} can be approximated by

$$P_e^{signal} \approx \overline{N}_R \frac{\log_2 M}{\log_2(N_T M)} \times \left\{\left[g\left(\frac{3(|\mu_T|-|\nu_T|)}{2(M-1)\sigma^2}\right)\right]^{N_R} + \frac{1/M}{\log_2 M}\left[g\left(\frac{M}{8}\times\frac{3(|\mu_T|-|\nu_T|)}{2(M-1)\sigma^2}\right)\right]^{N_R}\right\}, \quad (10)$$

where $(|\mu_T| - |\nu_T|)$ is the square root of the minimum eigenvalue of the matrix $\mathbf{B}^H\mathbf{B}$ and $\overline{N}_R = \frac{(2N_R-1)!}{N_R!(N_R-1)!}$.

2) $P_e^{spatial}$ results from summing all terms in Eq. (4) for which $i \neq i'$ and $l = l'$. Hence, the Hamming distance $d\left((i,l),(i',l')\right)$ and the random variable t are reduced to $d(i,i')$ and $t = \left\|\left(\overline{\mathbf{H}}_{eq}^{(i)} - \overline{\mathbf{H}}_{eq}^{(i')}\right)\mathbf{s}_l\right\|_2^2$, respectively. Hence, the MGF of the random variable t is given by $\Phi_t(\vartheta) = (1-2\vartheta\varphi_l)^{-N_R}$ where $\varphi_l = \|\mathrm{B}\mathbf{s}_l\|_2^2$. Recalling [12, Lemma 1], $P_e^{spatial}$ is given by

$$P_e^{spatial} = \frac{N_T}{2M}\frac{\log_2 N_T}{\log_2(N_T M)}\sum_{l=1}^{M}\beta\left(\frac{\varphi_l}{4\sigma^2}\right), \quad (11)$$

which can be approximated for high SNR by

$$P_e^{spatial} \approx \frac{1}{4}\overline{N}_R\frac{N_T\log_2 N_T}{M^2}\frac{\log_2 M}{\log_2(N_T M)} \times\left[g\left(\frac{3(|\mu_T|-|\nu_T|)}{2(M-1)\sigma^2}\right)\right]^{N_R}. \quad (12)$$

3) Finally, P_e^{joint} collects all the terms that are neither in P_e^{signal} nor $P_e^{spatial}$ in Eq. (4) for which $i \neq i'$ and $l \neq l'$. Based on [12, Lemma 1], the MGF of the random variable t is given by $\Phi_t(\vartheta) = (1-\vartheta(\varphi_l+\varphi_{l'}))^{-N_R}$ where the parameter $\varphi_{l'} = \|\mathrm{B}\mathbf{s}_{l'}\|_2^2$. Hence, P_e^{joint} is given by, after some mathematical manipulations

$$P_e^{joint} = \frac{1}{M\log_2(N_T M)}\sum_{l=1}^{M}\sum_{l'\neq l}^{M} \times\left[\frac{N_T}{2}\log_2 N_T + (N_T-1)\,\mathrm{d}\left(l,l'\right)\right]\beta \left(\frac{(\varphi_l+\varphi_{l'})}{8\sigma^2}\right), \quad (13)$$

which can be approximated for high SNR by

$$P_e^{joint} \approx \frac{1}{2}\overline{N}_R\frac{\log_2 M}{\log_2(N_T M)} \times\left\{(N_T-1)\left[g\left(\frac{M}{16}\times\frac{3(|\mu_T|-|\nu_T|)}{2(M-1)\sigma^2}\right)\right]^{N_R} + \left((N_T-1)+\frac{N_T\log_2 N_T}{M^2}\right) \times\left[g\left(\frac{3(|\mu_T|-|\nu_T|)}{2(M-1)\sigma^2}\right)\right]^{N_R}\right\}, \quad (14)$$

Therefore, the union bound in Eq. (4) can be re-written as

$$P_e \leq P_e^{signal} + P_e^{spatial} + P_e^{joint}. \quad (15)$$

A. Comparison With Single-Antenna Transmission

For any transmission scheme X, the BER $P_{e,X}$ can be expressed as $P_{e,X} = K_X(SNR_X)^{-N_R}$ [10]. For any two transmission schemes X and Y, the SNR difference (in dB) between X and Y to achieve the same BER $P_{e,X} = P_{e,Y}$ [10] is defined as $\triangle_{SNR}^{X/Y} = -(10/N_R)\log_{10}(K_Y/K_X)$ [10]. If $\triangle_{SNR}^{X/Y} > 0$, then for the same BER, Y needs $\triangle_{SNR}^{X/Y}$ dB less transmit energy than X, *i.e.*, $\triangle_{SNR}^{X/Y}$ is the SNR loss of X with respect to Y.

- SNR loss of SM due to TX I/Q Imbalance

We denote the I/Q imbalance-aware SM scheme by X and the I/Q imbalance-free SM scheme by Y. Based on our BER analysis in Section III, the SNR loss of SM due to TX I/Q imbalance is given by

$$\triangle_{SNR}^{X/Y} = \triangle_{SNR,\,SM}^{X/Y} = -10\log_{10}(|\mu_T|-|\nu_T|) + \frac{10}{N_R}\log_{10}\left(1+\left(\frac{N_T}{2^m}\right)\frac{\left(2^{m-3}/N_T\right)^{-N_R}}{m-\log_2(N_T)}\right) - \frac{10}{N_R}\log_{10}\frac{K_X}{K_Y}, \quad (16)$$

where, for a spectral efficiency m (bps/Hz),

$$K_X = 1+\frac{N_T^3}{4^m}\log_2 N_T + (N_T-1)\left(\left(2^{m-4}/N_T\right)^{-N_R}+2^{-N_R}\right) \quad (17)$$

$$K_Y = 1+\frac{3}{4}\frac{\frac{N_T^3}{4^m}\log_2 N_T}{1+\left(\frac{N_T}{2^m}\right)\frac{\left(2^{m-3}/N_T\right)^{-N_R}}{m-\log_2(N_T)}} + \frac{1}{2}\frac{(N_T-1)\left(\left(\left(2^{m-4}/N_T\right)\right)^{-N_R}+2^{-N_R}\right)}{1+\left(\frac{N_T}{2^m}\right)\frac{\left(2^{m-3}/N_T\right)^{-N_R}}{m-\log_2(N_T)}}. \quad (18)$$

Therefore, the SNR loss $\triangle_{SNR,\,SM}^{X/Y}$ in Eq. (16) is decomposed into the following three components;

- the first term quantifies the impact of TX I/Q imbalance and is positive as $(|\mu_T|-|\nu_T|) < 1$;
- the second term depends only on the signal domain;
- the third term depends on both the signal and the spatial domain and is negative as $K_X > K_Y$.

Moreover, for high spectral efficiency m, the second term in Eq. (16) becomes negligible and the SNR loss $\triangle_{SNR,\,SM}^{X/Y}$ in Eq. (16) can be approximated as follows

$$\triangle_{SNR,\,SM}^{X/Y} \approx -10\log_{10}(|\mu_T|-|\nu_T|) - \frac{10}{N_R}\log_{10}(1+K_c), \quad (19)$$

where the design parameter K_c is given by

$$K_c = \frac{(N_T-1)\left(\left(\frac{2^{m-4}}{N_T}\right)^{-N_R}+2^{-N_R}\right)}{2+(N_T-1)\left(\left(\frac{2^{m-4}}{N_T}\right)^{-N_R}+2^{-N_R}\right)}. \quad (20)$$

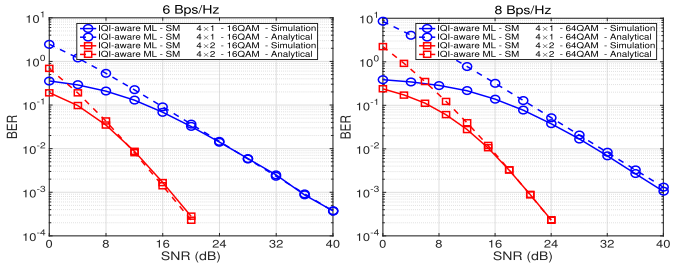

Fig. 1. SM BER performance comparison between analytical union bound in Eq. (15) and its numerical results for $N_R = 1, 2$ and $N_T = 4$ at a spectral efficiency of 6 bps/Hz and 8 bps/Hz.

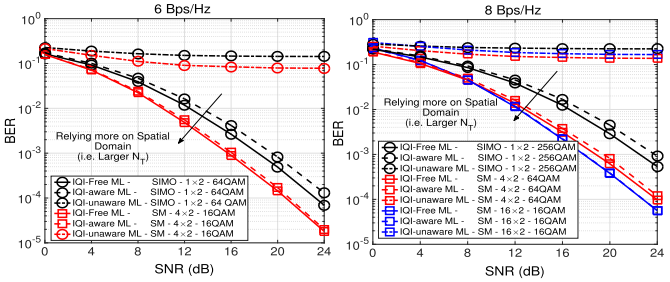

Fig. 2. BER performance comparison between SM and conventional SIMO at a spectral efficiency of 6 bps/Hz and 8 bps/Hz for $N_R = 2$.

Hence, in SM, the system designer has the additional flexibility due to the second term in Eq. (19) to jointly select N_T and M to achieve a high spectral efficiency $m = \log_2(N_T M)$ while still reducing the SNR loss due to TX I/Q imbalance below the first term in Eq. (19) which is not the case for conventional SIMO transmission as shown later on in this section.[1] For a given N_R and signal constellation size $M = 2^m/N_T$, the second term in Eq. (19) increases monotonically with N_T (more dependence on the spatial domain), which reduces the SNR loss due to TX I/Q imbalance until the second term asymptotically converges to $3/N_R$ (in dB). The result in Eq. (16) and its approximation in Eq. (19) show that, for high spectral efficiency m, relying more on the spatial domain (i.e. larger N_T), reduces the SNR loss due to TX I/Q imbalance.

- SNR loss of conventional SIMO transmission.
  Here, we denote the I/Q imbalance-aware conventional SIMO by scheme X and the I/Q imbalance-free conventional SIMO by scheme Y. The SNR loss due to TX I/Q imbalance for conventional SIMO is given by

$$\triangle_{SNR}^{X/Y} = \triangle_{SNR,\,SIMO}^{X/Y} = -10\log_{10}\left(|\mu_T| - |\nu_T|\right) + \frac{10}{N_R}\log_{10}\left(1 + \frac{\left(2^{m-3}\right)^{-N_R}}{m2^m}\right). \quad (21)$$

For high spectral efficiency m, we have

$$\triangle_{SNR,\,SIMO}^{X/Y} \approx -10\log_{10}\left(|\mu_T| - |\nu_T|\right), \quad (22)$$

which is higher than the SNR loss of SM in Eq. (19). This result unveils the robustness of SM-based transmission to TX I/Q imbalance compared to conventional SIMO.

IV. Numerical Results

We set the transmit side amplitude and phase imbalances to 1dB and 5°, respectively. In Fig. 1, we compare the BER union bound under TX I/Q imbalance (IQI) given by Eq. (15) with the BER simulated results for $N_R = 1, 2$ and $N_T = 4$ at spectral efficiencies of $m = 6$ bps/Hz and $m = 8$ bps/Hz. It can be seen that the upper bound becomes very tight with increasing SNR which demonstrates the accuracy of our analysis.

For a given spectral efficiency m, Fig. 2 demonstrates that, for SM, relying more on the spatial domain (i.e. increasing N_T), allows the system designer to reduce the SNR loss due to TX I/Q imbalance. In addition, we verified that our derived SNR loss expressions in Eqs. (16)-(22) match the numerical results in Fig. 2. Finally, Fig. 2 demonstrates that, at a given spectral efficiency m, the SNR loss due to TX I/Q imbalance in SM is less than its value in SIMO and SM outperforms SIMO both with and without TX I/Q imbalance which motivates its use for low-power IoT devices.

[1]Since SM is a single-RF transmission, we compare it with SIMO transmission for fairness

V. Conclusions

We derived an expression for the SNR loss of ML-based SM receivers due to TX I/Q imbalance as a function of its spectral efficiency, the TX I/Q imbalance parameters, and the number of transmit and receive antennas. Our analysis and numerical results demonstrate that, at a given spectral efficiency, relying more on the spatial domain (i.e. increasing N_T) for SM enhances its robustness to TX I/Q imbalance compared to conventional SIMO transmission. An interesting and challenging future extension is the case of spatial modulation with multiple active transmit antennas. Moreover, it is important to emphasize that our analysis can be easily extended to the case of colored Gaussian interference which can be used to model residual interference for a single-user detector at the data sink.

References

[1] Qualcomm Technologies Inc., "5G waveform & multiple access techniques," San Diego, CA, USA, Tech. Rep., Jul. 2015.
[2] M. Di Renzo *et al.* "Spatial modulation for generalized MIMO: Challenges, opportunities, and implementation," *Proc. IEEE*, vol. 102, no. 1, pp. 56–103, Jan. 2014.
[3] F. Horlin and A. Bourdoux, *Digital Compensation for Analog Front-Ends*. Hoboken, NJ, USA: Wiley, 2008.
[4] R. Mesleh *et al.*, "Impact of IQ imbalance on the performance of QSM multiple-input–multiple-output system," *IET Commun.*, vol. 10, no. 17, pp. 2391–2395, Nov. 2016.
[5] A. Afana and S. Ikki, "Analytical framework for space shift keying MIMO systems with hardware impairments and co-channel interference," *IEEE Commun. Lett.*, vol. 21, no. 3, pp. 488–491, Mar. 2017.
[6] L. Smaini, *RF Analog Impairments Modeling for Communication Systems Simulation: Application to OFDM-Based Transceivers*, 1st ed. Hoboken, NJ, USA: Wiley, 2012.
[7] A. Tarighat *et al.*, "Compensation schemes and performance analysis of IQ imbalances in OFDM receivers," *IEEE Trans. Signal Process.*, vol. 53, no. 8, pp. 3257–3268, Aug. 2005.
[8] A. G. Helmy *et al.*, "Enhanced-reliability cyclic generalized spatial-and-temporal modulation," *IEEE Commun. Lett.*, vol. 20, no. 12, pp. 2374–2377, Dec. 2016.
[9] M. K. Simon and M.-S. Alouini, *Digital Communication Over Fading Channels*, 2nd ed. Hoboken, NJ, USA: Wiley, 2005.
[10] M. Di Renzo and H. Haas, "Bit error probability of SM-MIMO over generalized fading channels," *IEEE Trans. Veh. Technol.*, vol. 61, no. 3, pp. 1124–1144, Mar. 2012.
[11] A. Hedayat *et al.*, "Analysis of space-time coding in correlated fading channels," *IEEE Trans. Wireless Commun.*, vol. 4, no. 6, pp. 2882–2891, Nov. 2005.
[12] M.-C. Lee *et al.*, "BER analysis for spatial modulation in multicast MIMO systems," *IEEE Trans. Commun.*, vol. 64, no. 7, pp. 2939–2951, Jul. 2016.